PROCESS PLANNING AND CONTROL FOR FUNCTIONALLY GRADED MATERIAL FABRICATION USING FREEZE-FORM EXTRUSION FABRICATION

Brad Deuser, Lie Tang, Jeff Geldmeier, Robert G. Landers, and Ming C. Leu

Department of Mechanical and Aerospace Engineering
Missouri University of Science and Technology, Rolla, MO 65409

REVIEWED, August 17 2011

Abstract

Using multiple materials in additive manufacturing technologies is critical for building parts with functionally gradient geometries. In order to achieve a desired material gradient, an advanced process planning and control system is required. This paper details the development of a process planning method and control system for functionally graded material fabrication using a triple extruder Freeze-form Extrusion Fabrication (FEF) system including motion code generation, extruder dynamic modeling and control, and composition gradient control. The effect that extruding multiple materials from a single orifice via static mixing has on the time delay of the resulting mixture is taken into account for path planning, and this factor is incorporated into integrating motion codes with extrusion commands. The effectiveness of the proposed system is demonstrated by fabricating three-dimensional parts with desired gradient compositions using multiple materials.

Introduction

Additive manufacturing (AM) technology has advanced past the phase of rapid prototyping since its inception in the late 1980s and continues to evolve with the addition of novel building materials, advanced control schemes and the ability to fabricate intricate parts with complex internal cavities. These features, in combination with increasing machine efficiency and little to no material waste, make AM technology desirable for building serviceable parts which are difficult and sometimes impossible to produce using traditional subtractive manufacturing processes. Among these advancements is the capability to build parts with multiple materials and functionally graded material (FGM) geometries.

Many attempts have been made by researchers to apply material composition gradients to solid CAD models using novel approaches such as heterogeneous object modeling [1], equal distance offset approach [2], and local composition control [3]. These methods decompose CAD models into their hierarchal elements in order to apply either material composition information to specific geometric features, or to apply graded material compositions through the cross section of a part. However, our project's initial efforts have focused on a simplified approach, which involves manipulating tool path motion codes generated by proprietary software (Stratasys Insight). This software is capable of generating tool path information for additive manufacturing applications with homogeneous materials, notably Fused Deposition Modeling (FDM) [4], but does not allow for multiple materials or functionally graded compositions. Therefore, in order to utilize this software, an algorithm was developed to integrate heterogeneous material composition gradient information with the pre-processed tool path from either Insight or a

manually written G&M code to be used by extrusion-based additive manufacturing processes such as the Freeze-form Extrusion Fabrication process we are researching.

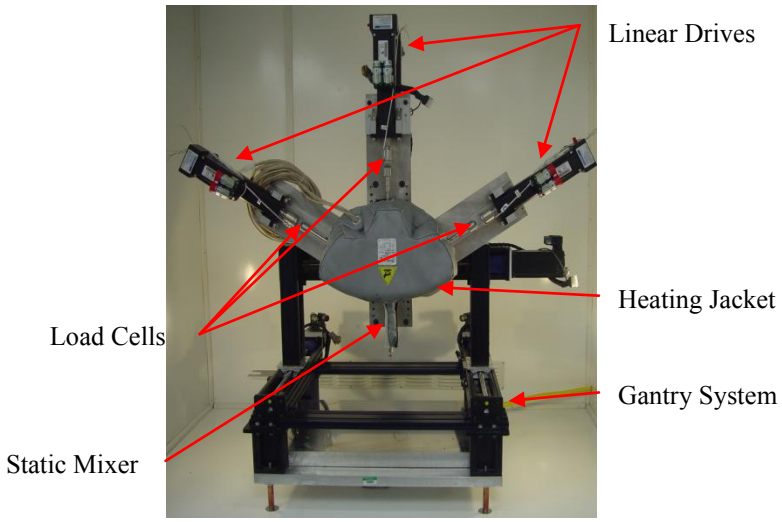

Figure 1: FEF machine with a triple-extruder mechanism.

Freeze-form Extrusion Fabrication (FEF) is a novel, layer-by-layer additive manufacturing process that builds three-dimensional (3D) parts by extruding aqueous-based colloidal pastes in an environment below the freezing point of water (-10° in our present study) in order to solidify the material as it exits the nozzle. This increases the build strength of each part and allows the FEF process to fabricate parts larger than that of room temperature extrusion processes (e.g., Robocasting [5] and Fab@Home [6]), and enables unsupported overhangs as much as 35° from the horizontal surface [7]. The triple-extruder FEF machine (Figure 1) is capable of depositing three separate pastes from a single orifice by using an inline static mixer to blend together multiple materials (Figure 2). This passive mixing technique has been used to minimize the number of moving components and controller complexity. However, it introduces a transport delay for changes in material composition that must be taken into account by the path planning software.

Figure 2: Static mixer (left) with mixing elements (right).

The research detailed in this paper outlines key issues for fabricating parts with multiple materials using the triple-extruder FEF system, which include: development of a general tracking velocity controller for the extrusion servo motors, taking into account the transport delay caused by the static mixer, and applying compositional gradients to the fabrication of a 3D part. An analytical model of the transport delay was devised and then verified through experimental results, and graded parts were built using the developed process planning algorithm.

FEF Equipment

The triple extruder FEF machine is comprised of two coupled mechatronic systems: motion control and extrusion control (Figure 3). The three-axis motion gantry system is controlled using a Delta Tau Turbo PMAC card, which operates the FEF machine through G&M motion code. Extrusion is controlled with three Kollmorgen servo motors (AKM23D) using a National Instruments PXI chassis and LabVIEW. The two systems are coupled by sending analog signals from the Delta Tau system to the PXI-6025E LabVIEW multifunction board, which interprets the voltage into different commands (namely, the reference velocity of each plunger and the start and stop commands for extrusion on demand [5]). The PXI-6025E multifunction board also acquires signals from three load cells (Omega LC-305), which are attached to the end of each linear motion cylinder. These load cells track the amount of pressure being exerted on the plunger and serve as a regulation feedback device for extrusion on demand, monitoring paste quality and detecting clogging or the presence of air bubbles at the nozzle tip. The PXI system also houses a counter/timer board (PXI-6022) for velocity tracking using encoder measurements in quadrature mode for a maximum resolution of 0.2 μm/s. The final component on the PXI system is the analog output board (PXI-6711), which sends command voltages to the three linear cylinder amplifiers.

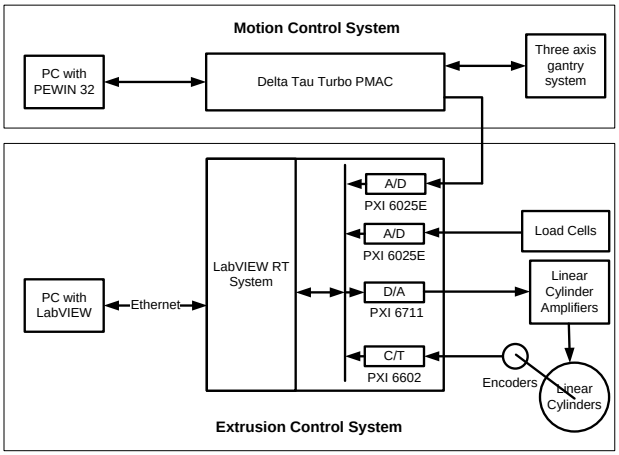

Figure 3: FEF control system schematic

Process Modeling and Control

Linear Cylinder Velocity Controller Design

Previous groups at Missouri S&T implemented extrusion force control to regulate the extrusion velocity [9-13] and achieved much success in doing so for a single-extruder FEF system. However, the triple-extruder FEF machine cannot use the same methodology because all three syringes deliver material through a single orifice, and the back pressure caused by advancing one plunger will affect the forces acting on the other cylinders. Given the already complex and limited nature of the adaptive control technique [9] and taking into consideration the possibility of multiple materials with different viscosities being extruded simultaneously, force control was not a viable option. In order to alleviate this issue, a general tracking controller was developed to run the linear cylinders with desired (reference) velocities. The linear cylinder dynamics are modeled as

$$\tau\dot{v} + v = Ku - f \tag{1}$$

where τ is the time constant (s), v is the plunger speed (mm/s), K is the gain (mm/s/V), u is the control voltage (V), and f is the friction (mm/s). To determine the model parameters, i.e., τ, K, and f, a pyramid command voltage signal is sent to the servo motor and the corresponding plunger speed is recorded. The model parameters then are determined using a particle swarm

optimization algorithm [14,15], which is an evolutionary computational technique based on swarm intelligence. In the particle swarm algorithm, the trajectory of each particle (i.e., set of candidate model parameters) in the search space is adjusted according to its own experience and the experience of the other particles in the swarm. The resulting model parameters are listed in Table 1. To demonstrate the model's performance, the simulated cylinder/plunger velocity using the developed model is compared with the measured velocity, as shown in Figure 4. The results demonstrate that the linear cylinder model fits the experimental data very well. A general tracking controller, as shown in Figure 5, is then designed to track the reference velocity v_r. The sampling period, T_s, is 0.01 s.

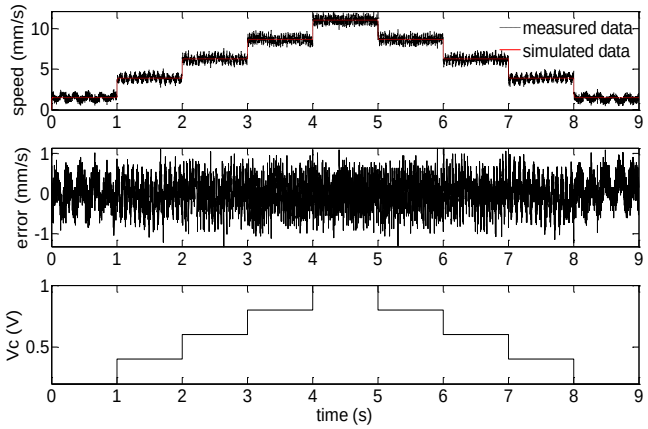

Figure 4: Comparison of the linear cylinder 1 velocity model and experimental results

Table 1: Linear cylinder parameters

Cylinder	τ (s)	K (mm/s/V)	f (mm/s)
1	$3.60 \cdot 10^{-3}$	11.95	0.934
2	$4.82 \cdot 10^{-3}$	11.81	1.056
3	$4.26 \cdot 10^{-3}$	11.62	1.022

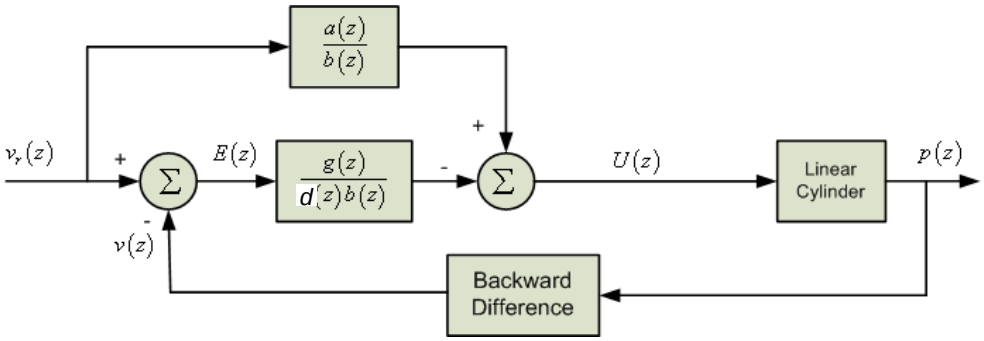

Figure 5: General tracking velocity controller

Here,

$$\frac{V(z)}{U(z)} = \frac{k\left(1-e^{-T/\tau}\right)}{z-e^{-T/\tau}} = \frac{b(z)}{a(z)} \tag{2}$$

and $d(z) = z-1$ in Figure 5 is the disturbance-generating polynomial. By including this polynomial, the Internal Model Principle is utilized to robustly reject constant disturbances such as Coulomb friction. The characteristic polynomial $d(z)a(z)-g(z)$ is designed to have two poles located at $-e^{-T_s/\tau_1}$ and $-e^{-T_s/\tau_2}$; thus, the controller polynomial $g(z)$ is

$$g(z) = g_1(z) + g_0 = \left(e^{-T_s/\tau_1} + e^{-T_s/\tau_2} - 1 - e^{-T_s/\tau}\right)z + \left(e^{-T_s/\tau} - e^{-T_s/\tau_1 - T_s/\tau_2}\right) \tag{3}$$

The control signal is

$$u(k) = u(k-1) + \frac{v_r(k+1) - \left(1+e^{-T_s/\tau}\right)v_r(k)}{K\left(1-e^{-T_s/\tau}\right)} + \frac{e^{-T_s/\tau}v_r(k-1) - g_1 e_v(k) - g_0 e_v(k-1)}{K\left(1-e^{-T_s/\tau}\right)} \tag{4}$$

where the speed error is

$$e_v(k) = v_r(k) - v(k) \tag{5}$$

Analytical Determination of Transport Delay

The system transport delay must be repeatable and accurately predicted in order for the path planning algorithm to deposit material in the desired location. The transport delay of the system *t* (sec) was modeled using linear relationships between the paste volumetric flow rate *Q* (m^3/sec) and the combined internal volume of each segment of the static mixer $\mathcal{V}$ (m^3). Variations in the paste's viscosity and compressibility, as well as the effects of gravity, were considered negligible, thus, the volumetric flow rates of pastes can be related to the time delay for steady state flow as follows:

$$t = \frac{\mathcal{V}}{\sum_{i=1}^{n} Q_i} \tag{6}$$

where *n* represents the number of cylinders being used. For the triple-extruder system, equation 6 becomes:

$$t = \frac{\mathcal{V}}{A_1 v_1 + A_2 v_2 + A_3 v_3} \tag{7}$$

where *A* (m^2) is the cross sectional area of the cylinder, and *v* (m/sec) is the plunger's velocity. The combined flow rate from all three extruders, *Q*, is equal to the sum of the individual flow rates, Q_1, Q_2 and Q_3. The ratio of Q_1:Q_2:Q_3 can be used to represent the ratio of the three pastes in the material composition. For example, to achieve a mixture of 50% each of paste one and paste two:

$$Q_1 : Q_2 : Q_3 = 0.5 : 0.5 : 0 \tag{8}$$

With constant volume in the static mixer, increasing plunger velocity results in less time delay required to change materials. However, the extruded length of paste remains unchanged for the same nozzle orifice. Thus a better approach for paste mixing is to reduce the volume of the static mixer as long as complete mixing of the pastes can be achieved.

Experimental Verification of Analytical Transport Delay

Experiments were performed to verify the analytical transport delay by recording the time taken to switch the deposition from one material to another. For example, paste in the first barrel was extruded until the extrusion force reached a steady state value, at which point the velocity of the first plunger v_1 was set to zero, and the velocity of the second plunger v_2 was set to the reference velocity. A time delay measurement was taken from the point at which the material was switched to the point at which the material appeared to fully transition into the next material. This transition takes place in 60 to 200 seconds in our observations and it occurs because the second material being extruded must clear out the previous material from the internal surface of the static mixer. As the paste travels along the sidewalls and elements of the mixer, some degree of intermixing will occur before a complete change of material takes place. The time required to begin the transition to the time required to fully transition into the next material accounts for approximately 15 to 30% of the total time delay in our observations. The time required from the beginning of the transition to halfway through the transition when compared to the theoretical time delay calculated from equation 7 for four different plunger velocities is shown in Figure 6.

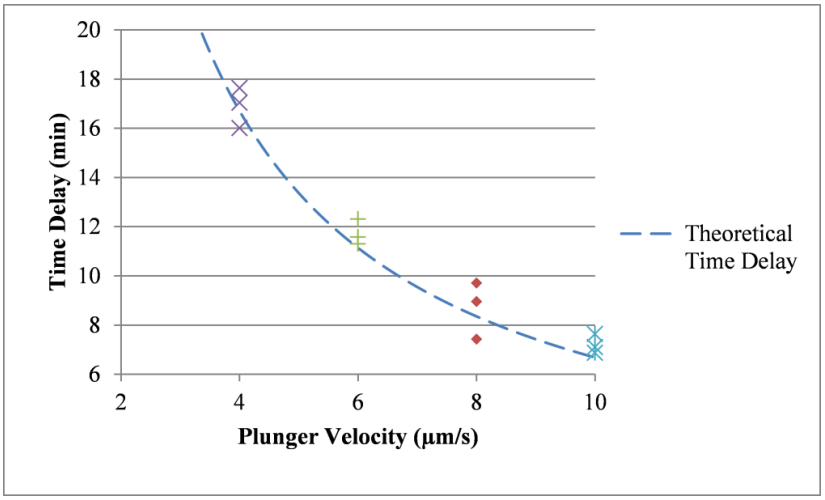

Figure 6: Experimental validation of the time delay model at four plunger velocities

The experimental results yield good accuracy for each plunger velocity when compared to the analytical predictions. For each velocity, the average of three runs comes within <4% of the theoretical time delay. One important factor in successful time delay repeatability is to ensure that the paste has been pre-loaded, or compressed, at the steady state force in each syringe prior to extrusion. For example, at a plunger velocity of 10 µm/s, the time delay averages seven minutes. When the target material was not pre-loaded to the steady state force (typically 600 N) prior to extrusion, delay times of up to fifteen minutes were observed. This increased delay has been thought to occur because the paste being used has some degree of compressibility which allows material from one syringe to enter the other if the two syringes are not both pre-loaded to

an equal force. This compressibility also adds error to the time delay measurements if the paste is not pre-loaded, by introducing a transient phase to the initial startup as the force ramps up to a steady state value. For continuous extrusion, this issue can be solved by maintaining a steady extrusion force for both cylinders. However, planning of tool paths for extrusion on demand (EOD), as required for most motion code programs must take this compressibility into account to avoid lengthening the time delay and facing the consequence of materials switching at an undesired location.

Control of Material Gradients

The algorithm developed to control the material gradient has two main functions: 1) implementing compensation for material transport delay and 2) applying material composition gradients to existing tool path motion code for homogeneous materials. The cylinder shown in Figure 7 was built by manually changing the velocity of each plunger to achieve a gradient from green to pink limestone ($CaCO_3$) paste in increments of 10% composition. In this case, G-code was written manually using circular arc functions, and the time delay was calculated and tested manually by varying the velocity of each plunger. The composition was varied by 10% every ten layers from the bottom (green) to the top (pink). It can be observed that composition increments near 10% for this height achieve a nearly continuous gradient over short distances from one material to the next. The goal of the gradient control algorithm is to automate this process for any geometry. In order to make the algorithm more versatile, it was designed to take in tool path information from both the Stratasys Insight software and generic G&M code to apply the transport delay and material gradients. With this functionality, primitive shapes such as plate or bar test specimens can be coded manually in G&M code and loaded into the program to apply the gradient and transport delay without having to model these simple shapes and go through the slicing and conversion process.

Figure 7: Cylinder with vertical gradient

Program Overview

The program was written in Mathworks Matlab 8, and its operation is outlined in Figure 8. It first reads in a text file output from Stratasys Insight, which includes tool path information in the format of Categorical Abstract Machine Language (CAML). Because motion control is executed through Delta Tau PEWIN software, tool path information must be translated into G&M coding language. Commands such as table speed (feed rate), extrusion status (on/off), and motion commands in the absolute positioning domain are extracted and converted. The resulting code is then modified to include Extrusion on Demand (EOD) commands and varying composition gradients by controlling the speed of each servo motor. With each incremental change in position, a corresponding distance traveled is associated with each set of two points. This distance is appended into an array and its cumulative distance is monitored to determine the current location within the 3D part being built. Lastly, changes in composition are modified to occur earlier by a factor determined by the time delay. This delay is expressed in the length of the material extruded as determined by multiplying the time delay t (sec) by the desired table

speed *s* (m/sec). The cumulative distance array is used to index the location of the gradient switch, and the new position within the code at which the change in velocity must take place is based on the transport delay. If the velocity must change before executing the motion code (e.g., if the composition is being changed near the beginning of a part), a DWELL command is sent to the controller to first carry out a purge cycle until the motion code can be run to achieve the desired gradient.

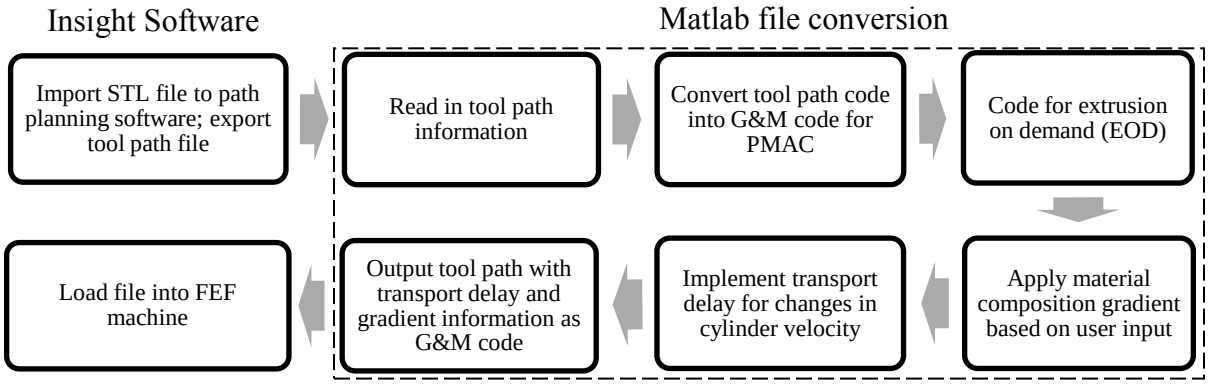

Figure 8: Schematic for Matlab program to apply multiple material compositions to the existing tool path code

Gradient Control Algorithm

Following the conversion to G&M code, the resulting tool path information is inserted into a matrix that includes the feed rate, M-code commands, coordinate information (X,Y,Z), incremental distance between each pair of coordinate points, the current layer, and any G-code commands. The feedrate is used to determine the time required for any necessary dwell commands. Coordinate information with corresponding distances and layers is used directly for the gradient control algorithm. All other parameters are simply passed through to be output to the final code. The primary transformation that takes place applies composition gradients in a user-defined orientation and increment (Figure 9) to the existing code. The first step in this process is to determine at what time to vary the velocity of each ram in order to achieve the desired gradient. The algorithm reads in each row to first acquire the cumulative distance traveled up to that point (CD). This is achieved by adding the incremental distance (D) from the previously calculated tool path matrix to the current distance. At the end of each layer the layer number (L_i) and length of extrudate on the current layer (CL_i) are output to a layer information matrix used by the gradient algorithm.

User input is required to first identify whether the gradient is to occur in the vertical or horizontal direction, which is used for raster path generated parts. In addition, a composition increment (ΔC) needs to be defined as a percentage of paste A to paste B (e.g., assuming even distributions, a composition increment of 25% would indicate that the part be split into five sections, with a composition of 0%B, 25%B, 50%B, 75%B and 100%B, respectively, from the beginning of the extrusion path to the end in the direction of the raster path).

Determination of vertical gradients is based on the total number of layers in a part (L_{total}). After being split into sections (ΔL) the tool path matrix is once again referenced within a loop and outputs a true case only if the current layer is divisible by the ΔL (e.g., if the composition changes every six layers, ΔL=6 and rem($L/\Delta L$) will equal 0 for layers 6, 12, …). If true, the distance required to switch materials (D_n) is calculated by taking the current cumulative distance (CD) and subtracting a transport delay (D_{delay}) for the current gradient (G_n). These values are output to a matrix referenced in a final transformation to apply motor velocity changes with an applied transport delay.

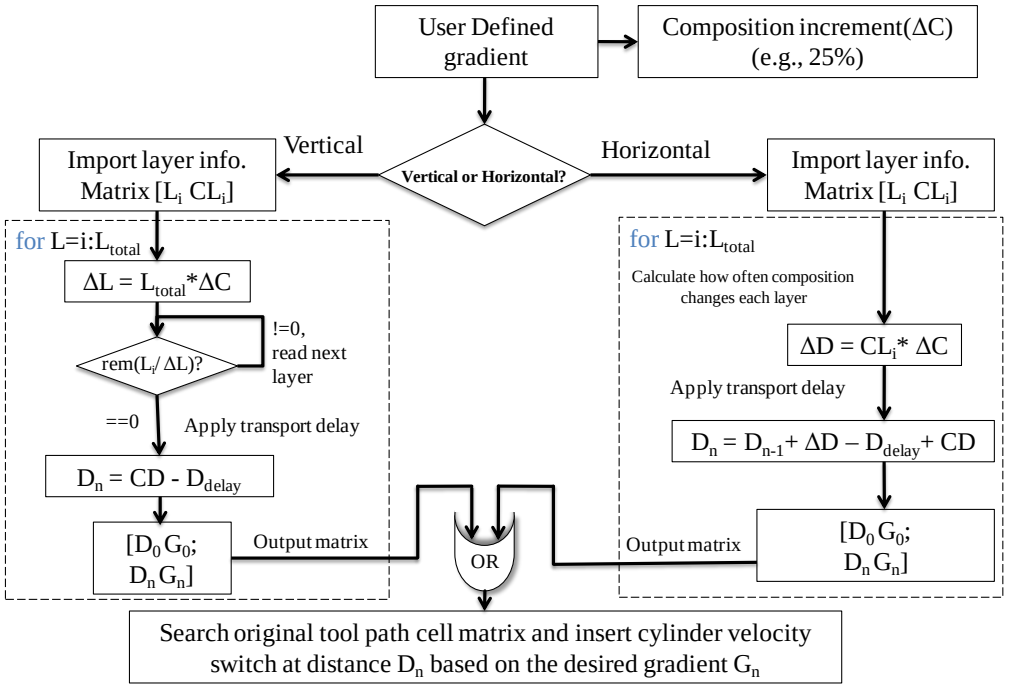

Figure 9: Gradient control algorithm schematic, where L=layer, D=distance, CD=cumulative distance, G=material gradient composition, CL=current layer, and D_{delay}=transport delay in terms of extruded length

Gradient Control Program Implementation

G-code Interpretation for Horizontal Gradients

Single-layer horizontal raster patterns were written in G-code to be 10.16 cm in width and 12.7 cm in length with a raster width of 1.27 mm. The same motion code was processed by the gradient control algorithm for three trials of grey-colored alumina paste (material A) to uncolored white alumina (material B) to switch compositions every 4.23 cm from 100%A to 100%B with a mixture of 50%(A+B) in the middle. The change in composition is marked by a region of transitional mixing (7.5 to 10 mm) and then there is a full switch to the desired ratio. This transition occurs over the span of 6 to 8 lines and accounts for 60.9 to 81.3 cm of extruded length at 6.35 mm/s table speed. Each test performed similarly with each composition change occurring within 42 cm of extruded length from the desired point of switching as seen in Figure 10.

To test the ability of the gradient control algorithm to plan composition changes for multiple layers, a 2.54 cm by 10 cm test bar was modeled using 3D CAD software and the final tool path code was tested with the FEF machine. Figure 11 shows the eighth layer of the test bar (4 mm in height), where the base layer is composed of 100% paste A and each subsequent layer contains a region to the right of 100% A (pink) and a region to the left of 100% B (green). Horizontal gradients showed repeatability from layer to layer within 1 cm in either direction for a total of eight layers. As mentioned previously, the transition region makes up 15-30% of the total time delay; therefore one limitation of the inline static mixer is a required minimal length for each layer in order to be able to fully transition from one material to the next. On average, for a plunger velocity of 10 μm/s, transitional mixing has been observed to take place in 81 cm or less. Since the overall length for each layer shown in Figure 11 is 203 cm, and 40% of the time extruding material is spent transitioning between paste A and paste B, only 30% of the part is pure A and 30% is pure B. This effect is undesirable for small parts, but larger parts may see some benefit from this transitional zone. For example, if two pastes composed of materials with different shrinkage rates are used to build a part, this transitional mixing will act as a buffer between composition changes to reduce the risk of delamination during the freeze-drying and sintering stages of post-processing. The pre-defined gradient could obviously be tailored such that drastic composition changes are avoided, but transitional mixing may add another level of protection to the green part and such complicated gradient schemes would not be necessary.

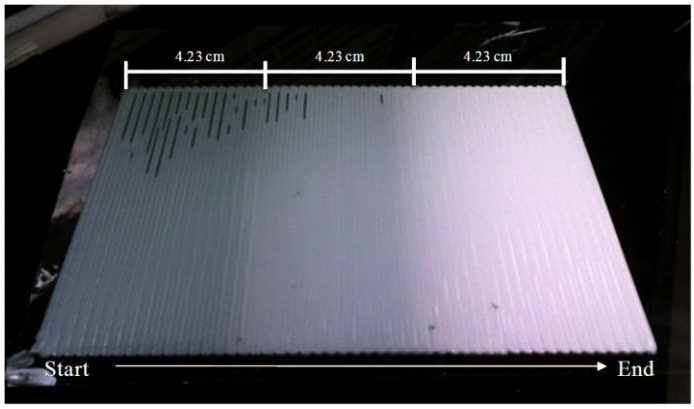

Figure 10: Transition from Al_2O_3 (gray) to Al_2O_3 (white), including a 50% mixing region.

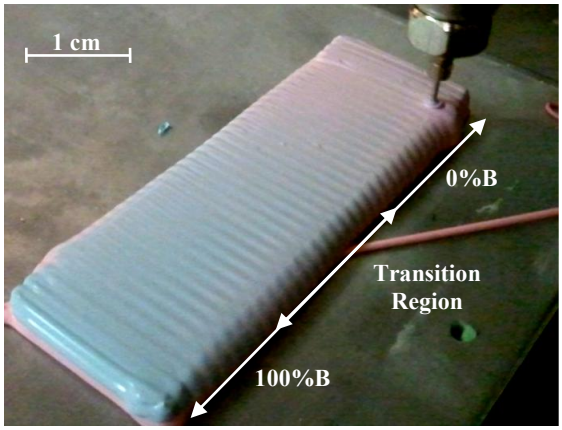

Figure 11: Eight-layer 2.54 cm by 10 cm block as the test bar.

G-code interpretation for Vertical Gradients

The vertical test bar shown in Figure 12 was produced using two pastes: 100% Alumina (paste A) and 50%Alumina-50%Zirconia (paste B). These tests were conducted to ensure the resulting mixture of paste A and paste B was of the correct composition. This part was built in an environment of -10°C from manually written G-code and automatically generated velocity control to vary the composition from 100% paste A ($100\%Al_2O_3$) for the first 20 layers to 50% paste A and 50% of paste B ($75\%Al_2O_3$-$25\%ZrO_2$) for the next 10 layers and 100% paste B ($50\%Al_2O_3$-$50\%ZrO_2$) for the final 10 layers. The part was freeze dried, sintered, cut and polished before applying a gold/palladium coating to condition the part for energy dispersive x-ray spectroscopy (EDS) measurements. Control pellets were manually mixed in precise measurements from the same alumina and alumina/zirconia pastes and sintered for comparison to the $75\%Al_2O_3$-$25\%ZrO_2$ mixture to ensure the correct composition was being achieved. EDS intensity measurements verified that the mixture of the two pastes mixed and deposited using the FEF process matched this composition from the control set by comparing the ratio of aluminum and zirconium from both sets of data.

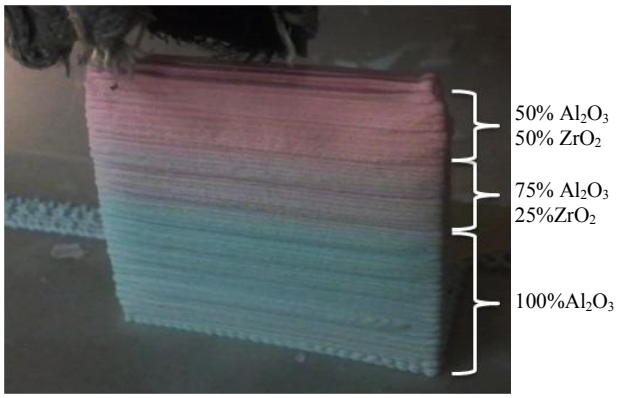

Figure 12: Alumina/Zirconia composite test part.

Conclusions

A machine code generation algorithm has been developed to implement a material transport delay and apply heterogeneous material compositions to existing G&M code for additive manufacturing of multiple materials using a triple-extruder Freeze-form Extrusion Fabrication (FEF) system. The generated motion code has been verified by depositing single- and multiple-layer horizontal gradients and multiple-layer vertical gradients. The transport delay caused by the use of an inline static mixer was taken into account by analytical methods and verified with empirical data and observation. Future work will include the expansion of gradient control such as radial gradients and coordinate-specific gradients, using all three extruders of the FEF system. Various process parameters will be optimized for the FEF machine for use with functionally graded parts. The sintering behavior of graded parts will be investigated, and the materials and mechanical properties of densified FGM parts will be tested to evaluate the effectiveness of the process.

Acknowledgements

This project is supported by NSF grant #CMMI-0856419, with participation and matching support of Boeing Company, through the Center for Aerospace Manufacturing Technologies at the Missouri University of Science and Technology, and by the Air Force Research Laboratory through Universal Technology Corporation (Contract #10-S568-0094-01-C1).

References

[1] X. Kou and S. Tan, "A Hierarchical Representation for Heterogeneous Object Modeling," Computer-Aided Design, Vol. 37, pp. 307-319, 2005.

[2] A. Xu and L. Shaw, "SFF-Oriented Modeling and Process Planning of Functionally Graded Materials using a Novel Equal Distance Offset Approach," Proceedings of Solid Freeform Symposium , Austin, TX, pp. 544-552, 2004.

[3] T. Jackson, N. Patrikalakis, E. Sachs and M. Cima, "Modeling and Designing Components with Locally Controlled Composition," Proceedings of Solid Freeform Symposium, Austin, TX, pp. 259-266, 1998.

[4] U.S. Pat. No. 5738817, April 14, 1998.

[5] J. Cesarano III, R. Segalmen, and P. Calvert, "Robocasting Provides Moldless Fabrication from Slurry Deposition," Ceramics Industry, Vol. 148, pp. 94-102, 1998.

[6] E. Malone and H. Lipson, "Fab@Home: the Personal Desktop Fabricator Kit," Rapid Prototyping Journal, Vol. 13, No. 4, pp. 245-255, 2007.

[7] X. Zhao, "Experimental Investigation of Effect of Environmental Temperature on Freeze-form Extrusion Fabrication," Thesis, Missouri University of Science and Technology, Rolla, MO, 2007.

[8] T. Oakes, P. Kulkarni, R. Landers, and M. Leu, "Development of Extrusion-on-Demand for Freeze-form Extrusion Fabrication Processes," Proceedings of the 3rd Annual ISC Research Symposium, Rolla, MO, 2009.

[9] Zhao, X., Landers, R.G., and Leu, M.C., 2010, "Adaptive Extrusion Force Control of Freeze–form Extrusion Fabrication Processes," ASME Journal of Manufacturing Science and Engineering, Vol. 132, No. 6, 064504.

[10] Mason, M.S., Huang, T., Landers, R.G., Leu, M.C., and Hilmas, G.E., "Aqueous–Based Extrusion of High Solids Loading Ceramic Pastes: Process Modeling and Control," Journal of Materials Processing Technology, Vol. 209, No. 6, pp. 2946–2957, 2009.

[11] M. Mason, T. Huang, M. Leu, R. Landers and G. Hilmas, "Aqueous-Based Extrusion Fabrication of Ceramics on Demand," Eighteenth Annual Solid Freeform Fabrication Symposium, Austin, TX, 2007.

[12] T. Huang, M. Mason, G. Hilmas, and M. Leu, "Aqueous Based Freeze-form Extrusion Fabrication of Alumina Components," Rapid Prototyping Journal, Vol. 15, No. 2, pp. 88-95, 2009.

[13] T. Huang, M. Mason, G. Hilmas, and M. Leu, "Freeze-form Extrusion Fabrication of Ceramic Parts," International Journal of Virtual and Physical Prototyping, Vol. 1, No. 2, pp. 93-100, 2006.

[14] J. Kennedy and R.C. Eberhart, "Particle Swarm Optimization," IEEE International Conference on Neural Networks, Perth, Australia, November 27–December 1, pp. 1942–1948, 1995.

[15] L. Tang, J. Ruan, R. Landers., and F. Liou, "Variable Powder Flow Rate Control in Laser Metal Deposition Processes," ASME Journal Manufacturing Science and Engineering, Vol. 130, No. 4, pp. 041016, 2008.